Construction of bi-functional inorganic–organic hybrid nanocomposites†

Suchetan Pal, Dinesh Jagadeesan, K. L. Gurunatha, M. Eswaramoorthy and Tapas Kumar Maji*

Received 20th June 2008, Accepted 2nd October 2008
First published as an Advance Article on the web 22nd October 2008
DOI: 10.1039/b810448d

Single system bi-functional inorganic–organic hybrid nanocomposites, PB@SiO_2@BTC@Ln (PB = Prussian blue, BTC = benzene tricarboxylate; Ln = Tb(III)/Sm(III)) having a PB magnetic core and a luminescent lanthanide probe, show superparamagnetic behavior and significant enhancement in luminescence intensities.

Inorganic magnetic nanoparticles (NPs) have been widely studied in recent years because of their high surface to volume ratio and high surface spins; they have applications in data storage, magnetic recording devices and biomedicine and are expected to be useful in future spintronics.[1] Nanocomposites with dual functionalities such as fluorescent-photostability and magnetism can be applicable in different advanced technologies, like magnetic resonance imaging of various biological systems including separation and detection of cancer cells,[2] bio-labeling[3] and bio-sensing.[4] Bi-functional composites consisting of a polymer coated Fe_2O_3 superparamagnetic core and a luminescent CdSe/ZnS quantum dots (QDs) shell or CdTe QDs on the surface were reported.[5] The presence of Cd in these systems severely restricts their use in medical and biological applications. Recently, Ln(III) ions have been used as an alternative emitting source material.[6] An inorganic–organic hybrid nanocomposite containing a magnetic inorganic core attached to light emitting Ln(III) ions through a organic linker may be a better substitute for Cd-containing quantum dots in many applications.[7,8] Prussian blue (PB) and its analogues composed of transition metal hexacyanometallates with the general composition of $A_i^{m+}[B(CN)_6]^{n-}$ are an important class of molecular magnet and exhibit versatile magnetic behavior depending on their constituents and ratios of transition metal ions.[9] In addition, the size and shape dependent magnetic properties exhibited by these materials[10] generated a great deal of interest in their synthesis at nanoscale dimensions. Mann *et al.* have reported the synthesis of hydrophobic PB nanoparticles in a reverse microemulsions technique[11] and later the synthesis and size dependent magnetic properties of PB nanoparticles using a homopolymer, poly(vinylpyrrolidine) (PVP), as a protective matrix was documented by Kitagawa *et al.*[12] In this communication, we report the design and synthesis of inorganic–organic hybrid nanocomposites, PB@SiO_2@BTC@Ln, with dual functionality combining the optical and magnetic properties associated with the magnetic PB core and the luminescent lanthanide (Tb(III) or Sm(III)) probe using silica spheres and an organic linker, benzene tricarboxylate (BTC).

The hybrid nanocomposite was fabricated in four steps (Scheme 1): (i) synthesis of PB nanoparticles using a PVP homopolymer matrix, (ii) coating of the PB nanoparticles with silica, (iii) attachment of the organic linker, BTC, on the silica surface, and finally, (iv) connecting of the Ln(III) ions with the resulting hybrid nanocomposite ligand. Here, we have used the silica coating for three reasons: it enhances the chemical stability[5,13] of the uncoated PB nanoparticles, surface silanol groups can covalently link with the different organic alcohol and acid molecules, and it can also produce stable dispersions in solvents having strong H-bonding affinity.

PVP protected PB nanoparticles were synthesized according to the procedure reported elsewhere (see ESI†).[12] A TEM image of the PB nanoparticles shows that the particle size are in range of 2–3 nm (Fig. S1†). The synthesized PB nanoparticles were coated with silica using the Stöber process, which is a well known method for silica coating.[14] The condensation rate of silica strongly depends upon the water content of the system and within 30 min the silica coating started to form around the PB nanoparticles. Vigorous stirring was continued throughout the reaction to ensure the uniform formation of the nanocomposites. The adsorbed PVP on the PB nanoparticles functions as a primer to promote the adhesion and condensation of silica. The IR spectrum of PB@SiO_2 shows four distinct bands around 1058 cm^{-1}, 1652 cm^{-1}, 2066 cm^{-1} and a broad absorption band around 3400 cm^{-1}, associated with ν(Si–O), ν(C═O) (from the amide carbonyl of PVP), ν(C≡N), and ν(O–H) stretching frequencies, respectively (Fig. S2†).[15] The broad band around 3400 cm^{-1} confirms the presence of a large number of –OH groups on the surface of the core/shell PB@SiO_2 nanoparticles. The PXRD pattern of PB@SiO_2 is shown in Fig. 1(a), which exhibits a similar pattern to that of the PB as well as PVP protected PB nanoparticles (ESI†).[16]

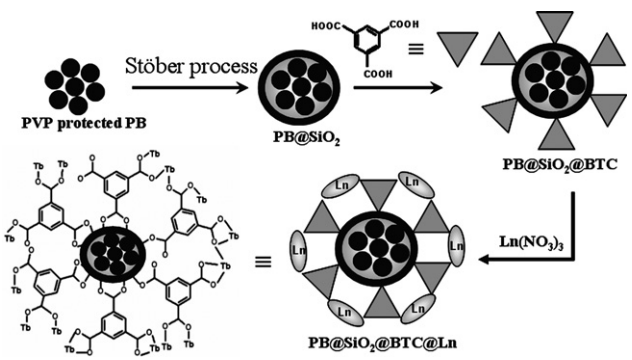

Scheme 1 Schematic diagram for the stepwise synthesis of inorganic–organic hybrid bi-functional nanocomposites PB@SiO_2@BTC@Ln (bottom left: the probable binding mode of the BTC with Ln(III) in hybrid nanocomposite).

Chemistry and Physics of Materials Unit, Jawaharlal Nehru Centre for Advanced Scientific Research, Jakkur, Bangalore, 560 064, India. E-mail: tmaji@jncasr.ac.in; Fax: +91-80-2208 2766; Tel: +91-80 2208 2826

† Electronic supplementary information (ESI) available: Experimental, synthesis of nanocomposites, FESEM, TEM images, IR, UV-Vis spectra. See DOI: 10.1039/b810448d

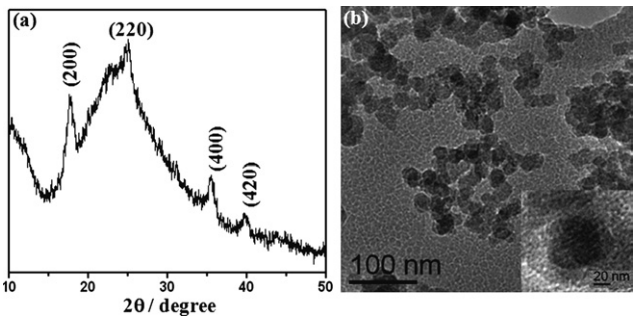

Fig. 1 Characterization of the as-synthesized silica coated PB nanoparticles: (a) PXRD pattern of PB@SiO_2; (b) high resolution TEM image of PB@SiO_2 (inset showing silica coated PB at a smaller scale).

The broad region between $2\theta = 20$–$30°$, which hides the 220 peak, indicates the presence of silica. TEM (Fig. 1b) and FESEM (Fig. S3†) images of the nanoparticles show spindle-like structures with particle sizes ranging from 20–25 nm (Fig. S4 and S5†). Considering the size of the individual PB particles which were around 2–3 nm, the silica coated PB nanoparticle is expected to have a silica shell thickness of about 10 nm. Occasionally, we have also found particles of size around 70 nm (inset Fig. 1b) having 30–40 nm PB core and about 20–30 nm silica shell thickness. This suggests a possible aggregation of PB nanoparticles before coating with the silica. EDX analysis suggests the presence of Fe, Si, C, N and O atom in the PB@SiO_2 nanocomposite.

The dispersion studies of PB@SiO_2 composite (about 1 mg) in different solvents shows that solvents having oxygen donor atoms, like H_2O, DMSO and THF, form stable dispersions while solvents like $CHCl_3$ form less stable dispersions (Fig. S6a†). This is probably due to the H-bonding interaction of the oxygen atom of the solvent with the surface –OH of the silica. The decrease in dispersability of silica coated PB nanoparticles compared to PVP protected PB nanoparticles (Fig. S6b†) further confirms that the PB nanoparticles are coated with silica. The change in the optical properties of the PB nanoparticles after silica coating is clearly seen from the UV-Vis spectra. When SiO_2 is coated on the PB nanoparticles, there is a blue shift from 700 nm to 680 nm (Fig. S7I†), due to the local refractive index around the particles increasing after the formation of the silica shell. The absorption is affected by the different solvents of different refractive indices, as evident from Fig. S7II.† With the increasing of refractive index, the PB peak around 700 nm becomes more pronounced.

The silica coated PB nanocomposites are now hybridized with the organic linker and luminescent Ln(III) ions. As carboxylic acid groups can covalently link with the silica surface, we have employed benzenetricarboxylic acid (BTC) as an organic linker. BTC has been proved to be a versatile linker towards Ln(III) due to its rigidity conferred by the benzene ring and structural flexibility due to the presence of three equally spaced carboxylate groups in three directions,[17] one of which can bind readily with the silica surface and other two available for binding with the Ln(III) ions. BTC molecules are attached to the surface of the silica as confirmed by UV-Vis spectra (Fig. S8†). BTC coated PB@SiO_2 exhibits an absorption peak around 206 nm in dispersion in aqueous medium after washing, which is similar to free BTC molecules in aqueous solution. The coordination mode of the carboxylate linker with the silica surface can be correlated from the IR bands in the range of 1340–1700 cm^{-1} (Fig. S9†).[15] Two strong and broad bands were observed at ~1641 cm^{-1} and ~1340 cm^{-1} corresponding to ν_{asym}(COO) and ν_{sym}(COO), respectively with the Δ value of 301 cm^{-1}, suggesting the unidentate binding of the BTC. There are also two strong bands at ~1565 (ν_{asym}) and ~1441 cm^{-1} (ν_{sym}) with the Δ value of 124 cm^{-1} indicating the presence of bidentate binding of the BTC to the silica surface. The peak around 1730 cm^{-1} corresponds to the presence of free uncoordinated –COOH groups available for binding with the Ln(III) ions. The PB@SiO_2@BTC hybrid nanocomposite was further linked with Ln(III) ions (Tb and Sm) in aqueous medium. There are several ways the BTC can bind to the Ln(III) ions (Schemes 1 and S1†); it can chelate, chelate and μ-oxo bridge, and even bind in a *syn–syn*, *syn–anti* or *anti–anti* bridging mode.[17] EDX analysis indicates the presence of Tb(III) and Sm(III) along with other components in the hybrid composite (Fig. S10†). The IR spectrum of PB@SiO_2@BTC@Tb/Sm shows no peak at ~1730 cm^{-1} for free –COOH, confirming their coordination with the Ln(III) ions.

UV-Vis spectra of the PB@SiO_2@BTC@Ln hybrid composites are given in Fig. S11† and emission spectra of BTC, free Ln(III) ions and hybrid nanocomposites are shown in Fig. 2. Free Tb(III) and Sm(III) ions exhibit very weak characteristic luminescence intensity in aqueous solution. The aqueous solution of $Tb(NO_3)_3$ shows peaks at

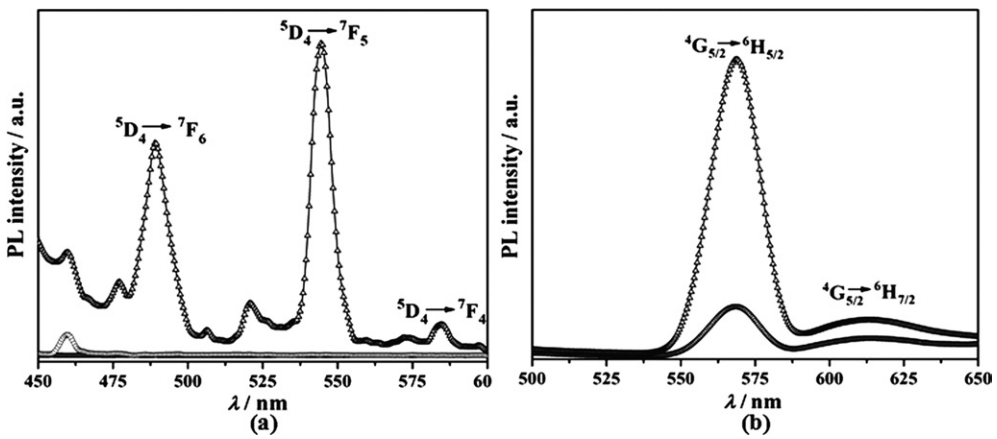

Fig. 2 Emission spectra: (a) PB@SiO_2@BTC@Tb (△), $Tb(NO_3)_3$ (○) and BTC (□) and (b) PB@SiO_2@BTC@Sm (△), $Sm(NO_3)_3$ (○).

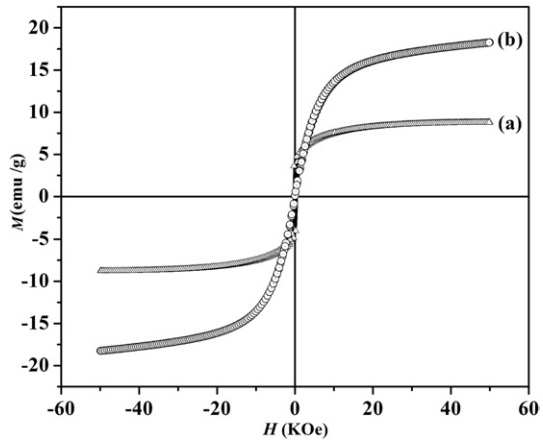

Fig. 3 Field dependent magnetization curves measured at 2.5 K: (a) PVP protected PB nanoparticles and (b) PB@SiO_2@BTC@Tb hybrid nanocomposite.

489 nm, 543.5 nm and 584.5 nm corresponding to $^5D_4$ to ^7F_J (J = 6, 5, 4) transitions.[18] When the Tb(III) loaded hybrid nanocomposite is excited at 300 nm, there is an abrupt enhancement of the luminescence intensity, which is much higher than for the free Tb(III) ions (Fig. 2a).[6] The excitation of the Sm(III) linked hybrid composite at 275 nm leads to the strong pink emission due to the $^4G_{5/2}$–^6H_J (J = 5/2 and 7/2) transitions. The intense peak is the transition $^4G_{5/2}$–$^6H_{5/2}$ at 568 nm and the other transition is $^4G_{5/2}$–$^6H_{7/2}$ at 611 nm, and the intensity is much higher than that of the corresponding free Sm(III) ions (Fig. 2b).[18] All the lanthanide ions have high affinity towards hard donors like oxygen and, therefore, PB@SiO_2@BTC@Ln hybrid nanocomposites show enhanced photo-luminescent properties due to the efficient energy transfer from the BTC linker to the bound Tb(III)/Sm(III).

In PB, three-dimensional long-range superexchange interactions between the neighboring Fe(III) ions (S = 5/2) through the NC–Fe(II)–CN linkages lead to ferromagnetic ordering at low temperature. Kitagawa *et al.* showed that with decreasing of the particle size, T_c also decreases in PVP coated PB nanoparticles, due to increasing surface to volume ratio.[12] The magnetic behavior with a smallest particle size to be superparamagnetic based on the nanoparticles with a single magnetic domain. We have studied the field dependent magnetization of the PB@SiO_2 and the PB@SiO_2@BTC@Tb inorganic–organic hybrid nanocomposites up to 5 T. The M *vs.* H plot is shown in Fig. 3, exhibiting the characteristic superparamagnetic behavior at 2.5 K, which is typical for magnetic nanoparticles. The magnetization value in the case of PB@SiO_2@BTC@Tb is increased significantly compared to PB@SiO_2, which is due to the presence of paramagnetic Tb(III) with S = 3. The atomic content of Tb(III) is 8.5% determined by EDX measurement, and is much higher than the Fe content of 2.83% in PB@SiO_2@BTC@Tb (Fig. S10†). Therefore, the large magnetization in the hybrid composite has a significant contribution from Tb(III) ions which are connected by the BTC linker.[18a]

We have synthesized and fabricated bi-functional PB@SiO_2@BTC@Ln that contain a PB magnetic core and luminescent Tb(III)/Sm(III) in one system using a silica coating. This method can be employed for the preparation of versatile bi-functional nanomaterials. The chemical stability of the hybrid nanocomposite is worth mentioning. Such bi-functional hybrid nanocomposites are addressable by a magnetic field and detectable from their characteristic photoluminescence properties. A significant increase is observed in the luminescence due to the ligand to metal energy transfer and is expected to serve as a luminescent marker in biological applications. We believe that this type of result will exhibit a new approach for utilizing the Prussian blue class of magnetic materials in advanced optical and magnetic applications.

The authors are thankful to Prof. C. N. R. Rao, FRS for the kind support and encouragement. The authors also acknowledge the DST Unit on Nanoscience, JNCASR, for FESEM facilities. S. Pal is grateful to JNCASR for SRFP.

Notes and references

1 (*a*) A.-H. Lu, E. L. Salabas and F. Schüth, *Angew. Chem. Int. Ed.*, 2007, **46**, 1222; (*b*) A. P. Alivistors, *Science*, 1996, **271**, 933; (*c*) C. T. Black, C. B. Murray, R. L. Sandstorm and S. Sun, *Science*, 2000, **290**, 1131; (*d*) S. Hashimoto, A. Maesaka, K. Fujimoto and K. Bessho, *Magn. Magn. Mater.*, 1993, **121**, 471; (*e*) A. K. Gupta and M. Gupta, *Biomaterials*, 2005, **26**, 3395.
2 (*a*) D. Artemov, N. Mori, B. Okollie and A. M. Bhujwalla, *Magn. Reson. Med.*, 2003, **49**, 403; (*b*) J.-H. Lee, Y.-M. Huh, Y. Jun, J. Seo, J. Jang, H.-T. Song, S. Kim, E.-J. Cho, H.-G. Yoon, J.-S. Suh and J. Cheon, *Nat. Med.*, 2007, **13**, 95; (*c*) A. Quarta, R. Di Corato, L. Manna, A. Ragusa and T. Pellegrino, *IEEE Trans. on NanoBioScience*, 2007, **6**, 298; (*d*) S. A. Corr, Y. P. Rakovich and Y. K. Gun'ko, *Nanoscale. Res. Lett.*, 2008, **3**, 87.
3 (*a*) Y. R. Chemla, H. L. Crossman, Y. Poon, R. Mcdermott, R. Stevens, M. D. Alper and J. Clarke, *Proc. Natl. Acad. Sci., USA*, 2000, **106**, 7177; (*b*) H. T. Song, J. Choi, Y.-M. Huh, S. Kim, Y. Jun, J.-S. Suh and J. Cheon, *J. Am. Chem. Soc.*, 2005, **127**, 9992; (*c*) Y.-M. Huh, E.-S. Lee, J.-H. Lee, Y.-W. Jun, P.-H. Kim, C.-O. Yun, J.-H. Kim, J.-S. Suh and J. Cheon, *Adv. Mater.*, 2007, **19**, 3109.
4 (*a*) D. R. Baselt, G. U. Lee, M. Natesan, S. W. Metzger, P. E. Sheehan and R. J. Colton, *Biosens. Bioelectron.*, 1998, **13**, 731; (*b*) S. T. Selvan, T. T. Tan and J. Y. Ying, *Adv. Mater.*, 2005, **17**, 1620.
5 (*a*) D. Wang, J. He, N. Rosenzweig and Z. Rosenzweig, *Nano Lett.*, 2004, **4**, 409; (*b*) N. Gaponic, I. L. Radtchenko, G. B. Sukhorukov and A. L. Rogach, *Langmuir*, 2004, **20**, 1449.
6 J. Choi, J. C. Kim, Y. B. Lee, I. S. Kim, Y. K. Park and N. H. Hur, *Chem. Commun.*, 2007, 1644.
7 (*a*) J. J. Yu, D. Parker, R. Pal, R. A. Poole and M. J. Cann, *J. Am. Chem. Soc.*, 2006, **128**, 2294; (*b*) C. Vancaeyzeele, O. Ornatsky, V. Baranov, L. Shein, A. Adelrahman and M. A. Winnik, *J. Am. Chem. Soc.*, 2007, **129**, 13653; (*c*) H. Mikola, H. Takkalo and I. Hemmilä, *Bioconj. Chem.*, 1995, **6**, 235.
8 (*a*) J. Massue, S. J. Quinn and T. Gunnlaugsson, *J. Am. Chem. Soc.*, 2008, **130**, 6900; (*b*) S. Comby, D. Imbert, C. Vandevyver and J.-C. G. Bunzli, *Chem. Eur. J.*, 2007, **13**, 936.
9 (*a*) S. Ferlay, T. Mallah, R. Quahes, P. Veillet and M. Verdaguer, *Nature*, 1995, **378**, 701; (*b*) O. Sato, T. Iyoda, A. Fujishima and K. Hashimoto, *Science*, 1996, **272**, 704; (*c*) S. Ohkoshi, Y. Abe, A. Fujishima and K. Hashimoto, *Phys. Rev. Lett.*, 1999, **62**, 1285; (*d*) H. S. Holmes and G. S. Girolami, *J. Am. Chem. Soc.*, 1999, **121**, 5593; (*e*) M. Ohba and H. Okawa, *Coord. Chem. Rev.*, 1998, **198**, 313.
10 (*a*) M. Cao, X. Wu, X. He and C. Hu, *Chem. Commun.*, 2005, 2241; (*b*) H.-L. Sun, H. Shi, F. Zhao, L. Qi and S. Gao, *Chem. Commun.*, 2005, 4339; (*c*) M. Yamada, M. Arai, M. Kurihara, M. Sakamoto and M. Miyake, *J. Am. Chem. Soc.*, 2004, **126**, 9482.
11 S. Vaucher, M. Li and S. Mann, *Angew. Chem. Int. Ed.*, 2000, **39**, 1793.
12 (*a*) T. Uemura and S. Kitagawa, *J. Am. Chem. Soc.*, 2004, **126**, 9482; (*b*) T. Uemura, M. Obha and S. Kitagawa, *Inorg. Chem.*, 2004, **43**, 7339.
13 (*a*) L. M. Liz-Marzán, M. Giersig and P. Mulvaney, *Langmuir*, 1996, **12**, 4329; (*b*) T. Ung, L. M. Liz-Marzán and P. Mulvaney, *Langmuir*, 1998, **14**, 3740; (*c*) C. R. Vestal and Z. J. Zhang, *Nano Lett.*, 2003, **12**, 1739; (*d*) M. P. B. van Bruggen, *Langmuir*, 1998, **14**, 2245.

14 (*a*) W. Stöber, A. Fink and E. Bohn, *J. Colloid Interface Sci.*, 1968, **26**, 62; (*b*) C. Graf, D. L. J. Vossen, A. Imhof and A. V. Blaaderen, *Langmuir*, 2003, **19**, 6693.
15 K. Nakamoto, *Infrared and Raman Spectra of Inorganic and Coordination compounds*, 5th ed; John Wiley & Sons; 1997.
16 H. J. Buser, D. Schwarzenbach, W. Petter and A. Ludi., *Inorg. Chem.*, 1977, **16**, 2704.
17 (*a*) C. Serre, F. Millange, C. Thouvenot, N. Gardant, F. Pelle and G. Ferey, *J. Mater. Chem.*, 2004, **14**, 1540; (*b*) N. L Rosi, J. Kim, M. Eddaoudi, B. Chen, M. O'Keeffe and O. M. Yaghi, *J. Am. Chem. Soc.*, 2005, **127**, 1504; (*c*) R. Gheorghe, P. Cucos, M. Andruh, J.-P. Costes, B. Donnadieu and S. Shova, *Chem.-Eur. J.*, 2006, **12**, 18721; (*d*) C. Daiguebonne, Y. Gerault, F. Le Dret, O. Guillou and K. Boubekeur, *J. Alloys Compd.*, 2002, **344**, 179.
18 (*a*) J. Xia, B. Zhao, H.-S. Wang, W. Shi, Y. Ma, H. B. Song, P. Cheng, D. Z. Liao and S.-P. Yan, *Inorg. Chem.*, 2007, **46**, 3450, and references therein; (*b*) Y.-G. Huang, B.-L. Wu, D.-Q. Yuan, Y.-Q. Xu, F.-L. Xiang and M.-C. Hong, *Inorg. Chem.*, 2007, **46**, 1171.